

OPTIMISATION METHODS FOR COMPUTATIONAL IMAGING

Chapter 2 - Variational approaches: From inverse problems to segmentation

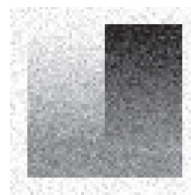
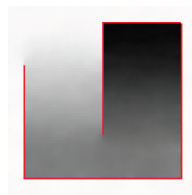
Nelly Pustelnik - ENS Lyon
Audrey Repetti - Heriot-Watt University

Journées SMAI-MODE 2022 – Limoges

Mumford-Shah (1989)

$$\underset{\mathbf{x}, K}{\text{minimize}} \quad \underbrace{\frac{1}{2} \int_{\Omega} (\mathbf{x} - \mathbf{z})^2 dx dy}_{\text{fidelity}} + \beta \underbrace{\int_{\Omega \setminus K} |\nabla \mathbf{x}|^2 dx dy}_{\text{smoothness}} + \underbrace{\lambda \mathcal{H}^1(K \cap \Omega)}_{\text{length}}$$

- ▶ Ω : image domain,
- ▶ $\mathbf{z} \in L^\infty(\Omega)$: input (possibly noisy),
- ▶ $\mathbf{x} \in W^{1,2}(\Omega)$: piecewise smooth approx. of \mathbf{z} ,
- ▶ K : set of discontinuities,
- ▶ \mathcal{H}^1 : Hausdorff measure.

 \mathbf{z}  $(\hat{\mathbf{x}}, \hat{K})$

Mumford-Shah (1989)

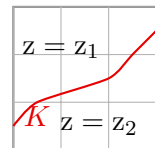
$$\underset{\mathbf{x}, K}{\text{minimize}} \quad \underbrace{\frac{1}{2} \int_{\Omega} (\mathbf{x} - \mathbf{z})^2 dx dy}_{\text{fidelity}} + \beta \underbrace{\int_{\Omega \setminus K} |\nabla \mathbf{x}|^2 dx dy}_{\text{smoothness}} + \underbrace{\lambda \mathcal{H}^1(K \cap \Omega)}_{\text{length}}$$

- ▶ Ω : image domain,
- ▶ $\mathbf{z} \in L^\infty(\Omega)$: input (possibly noisy),
- ▶ $\mathbf{x} \in W^{1,2}(\Omega)$: piecewise smooth approx. of \mathbf{z} ,
- ▶ K : set of discontinuities,
- ▶ \mathcal{H}^1 : Hausdorff measure.

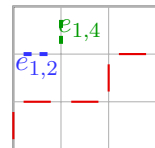
 \mathbf{z}  $(\hat{\mathbf{x}}, \hat{K})$

Discrete Mumford-Shah

$$\underset{\mathbf{x}, \mathbf{e}}{\text{minimize}} \frac{1}{2} \|\mathbf{x} - \mathbf{z}\|_2^2 + \beta \|(1 - \mathbf{e}) \odot \Psi \mathbf{x}\|^2 + \lambda \mathcal{R}(\mathbf{e})$$



\mathbf{x}_1	\mathbf{x}_4	\mathbf{x}_7
\mathbf{x}_2	\mathbf{x}_5	\mathbf{x}_8
\mathbf{x}_3	\mathbf{x}_6	\mathbf{x}_9



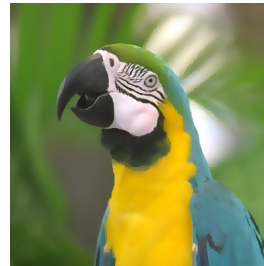
- ▶ $\Omega = \{1, \dots, N_1\} \times \{1, \dots, N_2\}$
- ▶ $\mathbf{z} \in \mathbb{R}^{|\Omega|}$: input (possibly noisy),
- ▶ $\mathbf{x} \in \mathbb{R}^{|\Omega|}$: piecewise smooth approx. of \mathbf{z} ,
- ▶ $\Psi \in \mathbb{R}^{|\mathbb{E}| \times |\Omega|}$: models a finite difference operator,
- ▶ $\mathbf{e} \in \mathbb{R}^{|\mathbb{E}|}$: edges between nodes whose value is 1 when a contour change is detected and 0 otherwise,
- ▶ \mathcal{R} : favors binary $\{0, 1\}^{|\mathbb{E}|}$ and sparse solution (i.e. “short $|K|$ ”).

Discrete Mumford-Shah

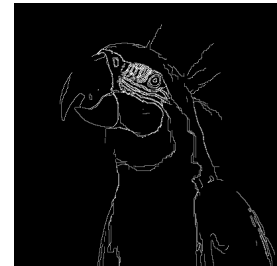
$$\underset{\mathbf{x}, \mathbf{e}}{\text{minimize}} \frac{1}{2} \|\mathbf{x} - \mathbf{z}\|_2^2 + \beta \|(\mathbf{1} - \mathbf{e}) \odot \Psi \mathbf{x}\|^2 + \lambda \mathcal{R}(\mathbf{e})$$



z



x̂



ê

Proposed Discrete Mumford-Shah

$$\underset{\mathbf{x}, \mathbf{e}}{\text{minimize}} \frac{1}{2} \|\mathbf{x} - \mathbf{z}\|_2^2 + \beta \|(\mathbf{1} - \mathbf{e}) \odot \Psi \mathbf{x}\|^2 + \lambda \mathcal{R}(\mathbf{e})$$

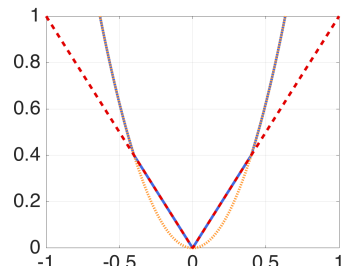
- Ambrosio-Tortorelli approximation:

[Ambrosio-Tortorelli, 1990][Foare-Lachaud-Talbot, 2016]

$$\mathcal{R}(\mathbf{e}) = \varepsilon \|\Psi \mathbf{e}\|_2^2 + \frac{1}{4\varepsilon} \|\mathbf{e}\|_2^2 \text{ with } \varepsilon > 0$$

- ℓ_1 -norm: $\mathcal{R}(\mathbf{e}) = \|\mathbf{e}\|_1$
- Quadratic ℓ_1 : [Foare-Pustelnik-Condat, 2017]

$$\mathcal{R}(\mathbf{e}) = \sum_{i=1}^{|\mathbb{E}|} \max \left\{ |e_i|, \frac{e_i^2}{4\varepsilon} \right\}.$$



Discrete Mumford-Shah like models

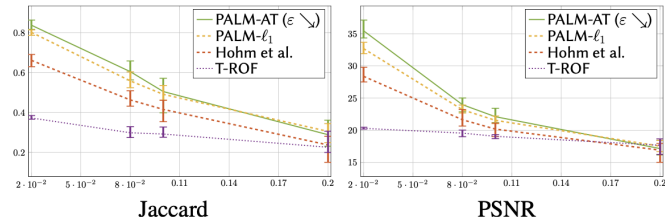
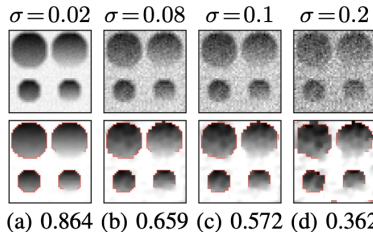
$$\underset{\mathbf{x}, \mathbf{e}}{\text{minimize}} \frac{1}{2} \|\mathbf{x} - \mathbf{z}\|_2^2 + \beta \|(\mathbf{1} - \mathbf{e}) \odot \Psi \mathbf{x}\|^2 + \lambda \mathcal{R}(\mathbf{e})$$

- **Two-step procedure:** $\hat{\mathbf{e}}$ extracted from

$$\hat{\mathbf{x}} = \underset{\mathbf{x}}{\operatorname{argmin}} \frac{1}{2} \|\mathbf{x} - \mathbf{z}\|_2^2 + \gamma P(\Psi \mathbf{x})$$

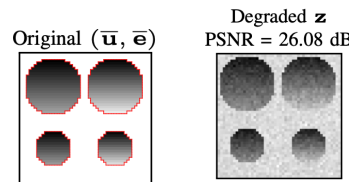
- ▶ Potts model (1952): $P(\cdot) = \|\cdot\|_0$ [Storath, Weinmann, 2014]
- ▶ Blake-Zisserman model (1987): $P(\cdot) = \sum_i \min(|(\cdot)_i|^q, \alpha^q)$ [Chambolle, 1995][Strelakowski, Cremers, 2014]
- ▶ TV denoising - ROF (1992): $P(\cdot) = \|\cdot\|_{2,1}$
 \Rightarrow Threshold-ROF (T-ROF) [Cai, Steidl, 2013]

Discrete Mumford-Shah models



[Le, Foare, Pustelnik, 2022]

Discrete Mumford-Shah models



	T-ROF [14]	Hohm et al. [12]	PALM- ℓ_1	SL-PAM- ℓ_1	PALM-AT $\epsilon=0.2$	SL-PAM-AT $\epsilon=0.2$	PALM-AT $\epsilon=2 \searrow 0.02$	SL-PAM-AT $\epsilon=2 \searrow 0.02$
$(\mathbf{u}^*, \mathbf{e}^*)$								
Jaccard	0.599	0.869	0.860	0.872	0.860	0.860	0.873	0.875
PSNR	30.5 dB	30.7 dB	27.5 dB	31.4 dB	30.1 dB	27.5 dB	34.2 dB	31.9 dB
CT	~ 10 sec.	~ 10 sec.	~ 10 sec.	~ 10 sec.	~ 1 min.	~ 1 h.	~ 10 min.	~ 1 h.

[Le, Foare, Pustelnik, 2022]

Total variation model

$$\underset{\mathbf{x}, K}{\text{minimize}} \frac{1}{2} \int_{\Omega} (\mathbf{x} - \mathbf{z})^2 dx dy + \beta \int_{\Omega \setminus K} |\nabla \mathbf{x}|^2 dx dy + \lambda \mathcal{H}^1(K \cap \Omega)$$

↓ Discrete piecewise constant relaxation

$$\underset{\mathbf{x}}{\text{minimize}} \frac{1}{2} \|\mathbf{x} - \mathbf{z}\|_2^2 + \lambda \text{TV}(\mathbf{x})$$

+ Convex.

+ Fast implementation due to strong convexity.

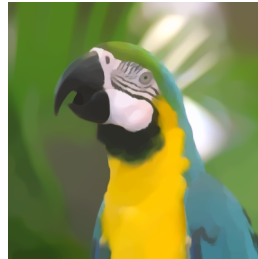
- TV denotes some form of the 2-D discrete total variation, i.e.,

$$(\forall \mathbf{x} \in \mathbb{R}^{|\Omega|}) \quad \text{TV}(\mathbf{x}) = \sum_{i_1=1}^{N_1} \sum_{i_2=1}^{N_2} \sqrt{|\mathbf{x}_{i_1+1, i_2} - \mathbf{x}_{i_1, i_2}|^2 + |\mathbf{x}_{i_1, i_2+1} - \mathbf{x}_{i_1, i_2}|^2}$$

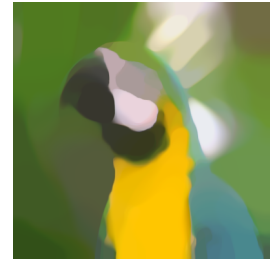
Total variation model



\mathbf{z}



$\hat{\mathbf{x}}_{\text{TV}}$ with $\lambda = 100$



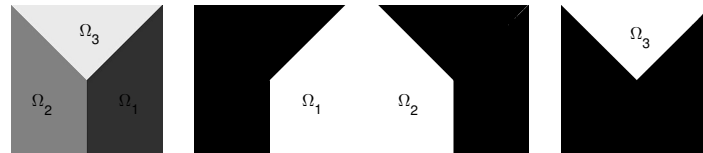
$\hat{\mathbf{x}}_{\text{TV}}$ with $\lambda = 500$

Chan-Vese model

$$\underset{\mathbf{x}, K}{\text{minimize}} \frac{1}{2} \int_{\Omega} (\mathbf{x} - \mathbf{z})^2 dx dy + \beta \int_{\Omega \setminus K} |\nabla \mathbf{x}|^2 dx dy + \lambda \mathcal{H}^1(K \cap \Omega)$$

Discrete piecewise constant relaxation with \downarrow fixed label number [Chan-Vese, 2001]

$$\min_{\boldsymbol{\theta}^{(q)}} \sum_{q=1}^Q \langle \boldsymbol{\theta}^{(q-1)} - \boldsymbol{\theta}^{(q)}, (\mu_q - \mathbf{z})^2 \rangle + \lambda \sum_{q=1}^Q \text{TV}(\boldsymbol{\theta}^{(q-1)} - \boldsymbol{\theta}^{(q)}) \text{ s.t. } 1 \equiv \boldsymbol{\theta}^{(0)} \geq \boldsymbol{\theta}^{(1)} \geq \dots \geq \boldsymbol{\theta}^{(Q-1)} \geq \boldsymbol{\theta}^{(Q)} \equiv 0,$$

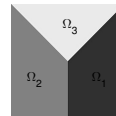


Chan-Vese model

$$\underset{\mathbf{x}, K}{\text{minimize}} \frac{1}{2} \int_{\Omega} (\mathbf{x} - \mathbf{z})^2 dx dy + \beta \int_{\Omega \setminus K} |\nabla \mathbf{x}|^2 dx dy + \lambda \mathcal{H}^1(K \cap \Omega)$$

Discrete piecewise constant relaxation with \downarrow fixed label number [Chan-Vese, 2001]

$$\min_{\boldsymbol{\theta}^{(q)}} \sum_{q=1}^Q \langle \boldsymbol{\theta}^{(q-1)} - \boldsymbol{\theta}^{(q)}, (\mu_q - \mathbf{z})^2 \rangle + \lambda \sum_{q=1}^Q \text{TV}(\boldsymbol{\theta}^{(q-1)} - \boldsymbol{\theta}^{(q)}) \text{ s.t. } 1 \equiv \boldsymbol{\theta}^{(0)} \geq \boldsymbol{\theta}^{(1)} \geq \dots \geq \boldsymbol{\theta}^{(Q-1)} \geq \boldsymbol{\theta}^{(Q)} \equiv 0,$$

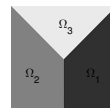
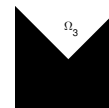
 \mathbf{z} $\boldsymbol{\theta}^{(0)}$ $\boldsymbol{\theta}^{(1)}$ $\boldsymbol{\theta}^{(2)}$ $\boldsymbol{\theta}^{(3)}$ 

Chan-Vese model

$$\underset{\mathbf{x}, K}{\text{minimize}} \frac{1}{2} \int_{\Omega} (\mathbf{x} - \mathbf{z})^2 dx dy + \beta \int_{\Omega \setminus K} |\nabla \mathbf{x}|^2 dx dy + \lambda \mathcal{H}^1(K \cap \Omega)$$

Discrete piecewise constant relaxation with \downarrow fixed label number [Chan-Vese, 2001]

$$\min_{\boldsymbol{\theta}^{(q)}} \sum_{q=1}^Q \langle \boldsymbol{\theta}^{(q-1)} - \boldsymbol{\theta}^{(q)}, (\mu_q - \mathbf{z})^2 \rangle + \lambda \sum_{q=1}^Q \text{TV}(\boldsymbol{\theta}^{(q-1)} - \boldsymbol{\theta}^{(q)}) \text{ s.t. } 1 \equiv \boldsymbol{\theta}^{(0)} \geq \boldsymbol{\theta}^{(1)} \geq \dots \geq \boldsymbol{\theta}^{(Q-1)} \geq \boldsymbol{\theta}^{(Q)} \equiv 0,$$

 \mathbf{z}  $\boldsymbol{\theta}^{(0)} - \boldsymbol{\theta}^{(1)}$  $\boldsymbol{\theta}^{(1)} - \boldsymbol{\theta}^{(2)}$  $\boldsymbol{\theta}^{(2)} - \boldsymbol{\theta}^{(3)}$

Chan-Vese model

$$\underset{\Theta = (\boldsymbol{\theta}^{(q)})_{1 \leq q \leq Q-1}}{\text{minimize}} \quad \sum_{q=1}^{Q-1} \langle \boldsymbol{\beta}^{(q)}, \boldsymbol{\theta}^{(q)} \rangle + \lambda \sum_{q=1}^Q \|DH_q \Theta\|_{2,1} + \iota_{[0,1]^{Q \times |\Omega|}}(\Theta) + \iota_E(\Theta)$$

- ▶ $\boldsymbol{\beta}^{(q)} = (\mu_{q+1} - \mathbf{z})^2 - (\mu_q - \mathbf{z})^2$,
- ▶ $H_q: \mathbb{R}^{Q \times |\Omega|} \rightarrow \mathbb{R}^{|\Omega|}: \Theta \mapsto \boldsymbol{\theta}^{(q-1)} - \boldsymbol{\theta}^{(q)}$,
- ▶ $E = \{\Theta \in \mathbb{R}^{Q \times |\Omega|} : \boldsymbol{\theta}^{(1)} \geq \dots \geq \boldsymbol{\theta}^{(Q-1)}\}$.

⇒ Use of splitting proximal algorithms to deal with a sum of convex but non-smooth functions.

Segmentation methods: summary

Discrete MS



Chan-Vese



Total Variation



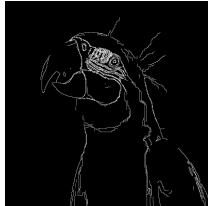
- + Extract contour
- + Identify smooth variations
- + Piecewise smooth
→ piecewise constant
- Time consuming
- Tune parameters

- + Perform good segmentation results
- + Fast
- Tune parameters: number of labels, mean value μ_q

- + Fast
- + Piecewise constant
- Not accurate contour

Segmentation methods: summary

Discrete MS



Chan-Vese



Total Variation

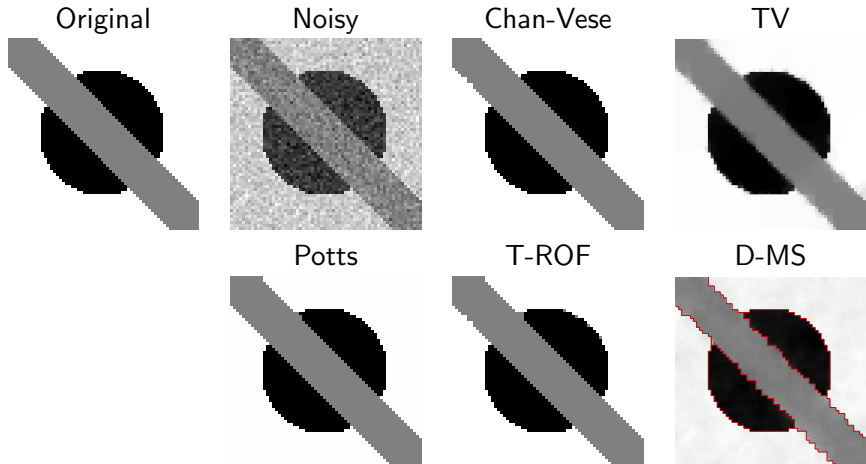


- + Extract contour
- + Identify smooth variations
- + Piecewise smooth
→ piecewise constant
- Time consuming
- Tune parameters

- + Perform good segmentation results
- + Fast
- Tune parameters: number of labels, mean value μ_q

- + Fast
- + Piecewise constant
- Not accurate contour

Discrete Mumford-Shah like models: visual comparisons

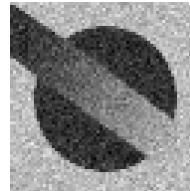


Discrete Mumford-Shah like models: visual comparisons

Original



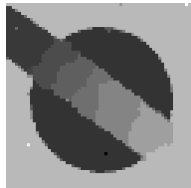
Noisy



Chan-Vese



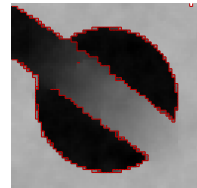
TV

Potts (small γ)Potts (large γ)

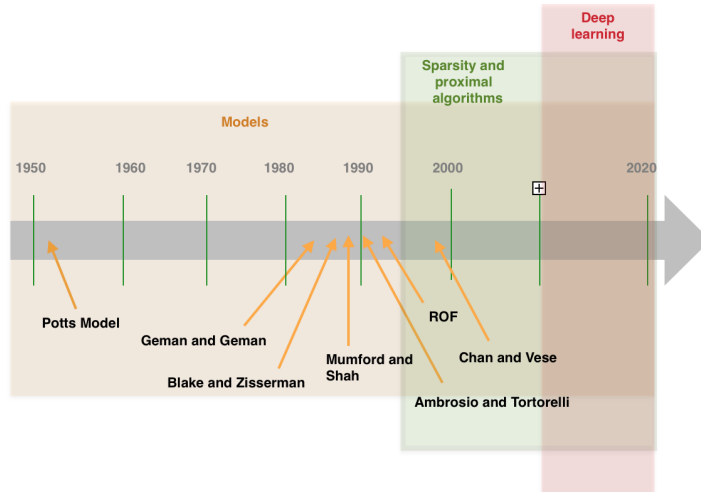
T-ROF



D-MS



Evolution of the models

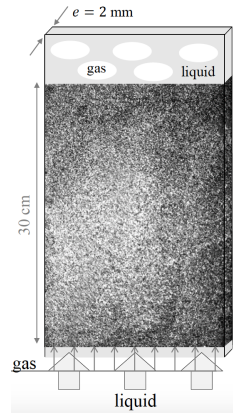
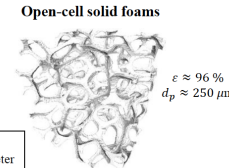
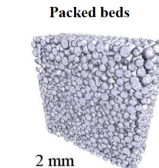


(Parameter-free and fast) texture segmentation

→ **LPENSL experiment:** joint gas and liquid flow through a porous medium

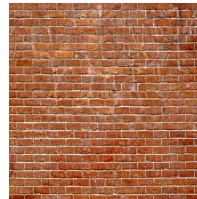
- Segment gas/liquid + accurate estimation of the interface.
- Large-scale data.

→ **Objective:** Study innovative material.

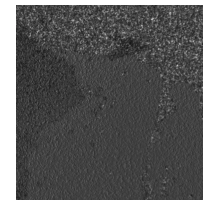
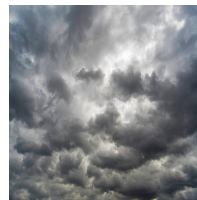


Stochastic textures

- Geometric textures → periodic

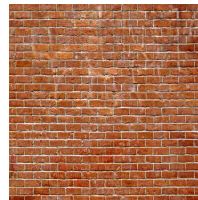


- Stochastic textures

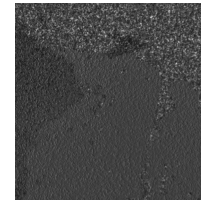
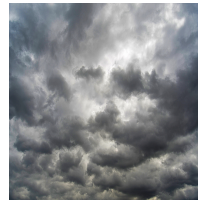


Stochastic textures

- Geometric textures → periodic

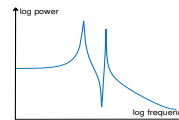
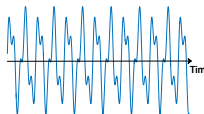


- Stochastic textures → scale-free ?

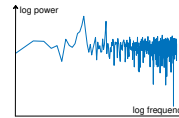


Stochastic textures

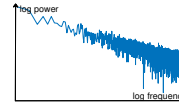
- Sinusoidal signal → periodic



- Sinusoidal signal + noise → periodic

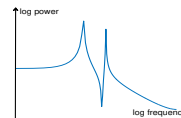


- Monofractal signal → scale-free

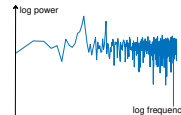


Stochastic textures

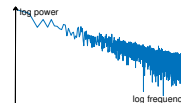
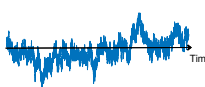
- Sinusoidal signal → periodic



- Sinusoidal signal + noise → periodic

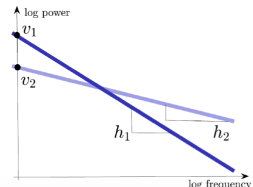
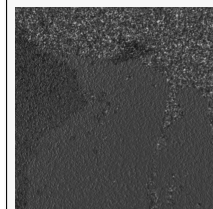


- Monofractal signal → scale-free



Texture segmentation:

→ require to compute the slope at each location.



(Parameter-free and fast) texture segmentation

→ Local regularity to characterize texture: [Jaffard, 2004][Wendt et al., 2009]

Wavelet coefficients

$$\zeta_j = \Psi_j \mathbf{z}$$

Wavelet leaders

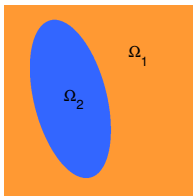
$$\mathcal{L}_{j,n} = \sup_{\lambda_{j',n'} \subset \Lambda_{j,n}} |\zeta_{j',n'}|$$

Behavior through the scales

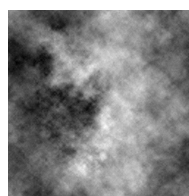
$$\mathcal{L}_{j,n} \simeq s_n 2^{jh_n} \text{ when } 2^j \rightarrow 0$$

Linear regression across scales

$$\hat{h}_n = \sum_j w_{j,n} \log_2 \mathcal{L}_{j,n}$$



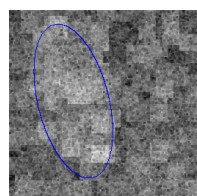
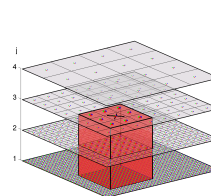
Mask



Original \mathbf{z}



$\zeta = D\mathbf{z}$



Estimate $\hat{\mathbf{h}}$

(Parameter-free and fast) texture segmentation

→ Linear regression across scales at each location:

$$\hat{h}_n = \sum_j w_{j,n} \log_2 \mathcal{L}_{j,n} \quad \text{with} \quad w_n \in C = \left\{ \sum_j w_{j,n} \equiv 0, \quad \sum_j j w_{j,n} \equiv 1 \right\}$$

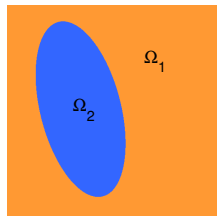
→ TV denoising: piecewise constant estimate:

$$\hat{h}_{\text{TV}} = \arg \min_h \frac{1}{2} \|h - \underbrace{\sum_j w_j \log_2 \mathcal{L}_j}_\text{h}\|_2^2 + \lambda \|\Psi h\|_{2,1}$$

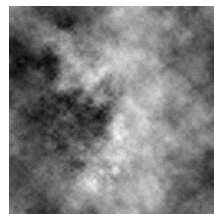
→ Joint estimation and segmentation:[Pustelnik, Wendt, Abry, Dobigeon, 2016]

$$(\hat{h}_{\text{TVW}}, \hat{w}) = \arg \min_{h,w} \frac{1}{2} \|h - \sum_j w_j \log_2 \mathcal{L}_j\|_2^2 + \lambda \|\Psi h\|_{2,1} + \|\mathbf{w} - P_C(\mathbf{w})\|_2^2$$

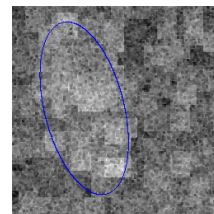
(Parameter-free and fast) texture segmentation



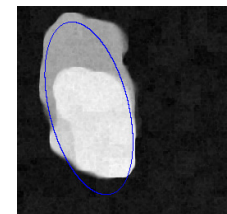
Mask



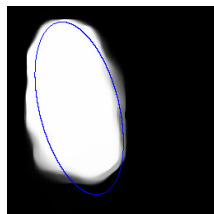
Original z



Estimate \hat{h}



Estimate \hat{h}_{TV}



Estimate \hat{h}_{TVW}

(Parameter-free and fast) texture segmentation



[Yuan et al. 2015]

Original z 

[Arbelaez et al. 2011]

 \hat{h}  \hat{h}_{TV} Estimate \hat{h}_{TVW}

(Parameter-free and fast) texture segmentation

→ Previous work [Pustelnik, Wendt, Abry, Dobigeon, 2016]

$$(\hat{h}_{TVW}, \hat{w}) = \arg \min_{h,w} \frac{1}{2} \|h - \sum_j w_j \log_2 \mathcal{L}_j\|_2^2 + \lambda \|\Psi h\|_{2,1} + \|w - P_C(w)\|_2^2$$

- + Good texture segmentation performance.
- + Convex minimization formulation.
- + Combined estimation and segmentation (contrary to \hat{h}_{TV}).
- Computational cost. Not adapted for large scale data.

(Parameter-free and fast) texture segmentation

→ Previous work [Pustelnik, Wendt, Abry, Dobigeon, 2016]

$$(\hat{h}_{TVW}, \hat{w}) = \arg \min_{h,w} \frac{1}{2} \|h - \sum_j w_j \log_2 \mathcal{L}_j\|_2^2 + \lambda \|\Psi h\|_{2,1} + \|w - P_C(w)\|_2^2$$

→ Behavior through the scales: $\mathcal{L}_{j,n} \simeq s_n 2^{jh_n}$ when $2^j \rightarrow 0$

$$\log_2 \mathcal{L}_{j,k} \simeq \underbrace{\log_2 s_n}_{v_n} + j h_n$$

→ New objective function [Pascal, Pustelnik, Abry, 2021]

$$(\hat{h}, \hat{v}) \in \operatorname{Argmin}_{h,v} \frac{1}{2} \sum_j \underbrace{\|v + jh - \log_2 \mathcal{L}_j\|_2^2}_{f(v,h;\mathcal{L})} + \lambda \left\| [\Psi h; \alpha \Psi v]^\top \right\|_{2,1}$$

Focus on the data-fidelity term

$$\begin{aligned} f(\mathbf{v}, \mathbf{h}; \mathcal{L}) &= \frac{1}{2} \sum_j \|\mathbf{v} + j\mathbf{h} - \log_2 \mathcal{L}_j\|_2^2 \\ &= \frac{1}{2} \sum_{\underline{n}} \sum_j (v_{\underline{n}} + j h_{\underline{n}} - \log_2 \mathcal{L}_{j,\underline{n}})^2 \\ &= \frac{1}{2} \sum_{\underline{n}} \left\| \Phi \begin{pmatrix} v_{\underline{n}} \\ h_{\underline{n}} \end{pmatrix} - \log_2 \mathcal{L}_{\underline{n}} \right\|_2^2 \quad \text{where } \Phi = \begin{pmatrix} 1 & 1 \\ 1 & 2 \\ \vdots & \vdots \\ 1 & J \end{pmatrix} \end{aligned}$$

→ Specificities

- Closed form expression of the associated proximity operator.
- Strongly convex.
- Closed form expression of the conjugate.

Focus on the data-fidelity term

Closed form for prox_f [Pascal, Pustelnik, Abry, 2021]

For every $(v, h) \in \mathbb{R}^{|\Omega|} \times \mathbb{R}^{|\Omega|}$, denoting $(p, q) = \text{prox}_f(v, h) \in \mathbb{R}^N \times \mathbb{R}^N$ one has

$$\begin{cases} p = \frac{(1+R_2)(\mathcal{S}+v)-R_1(\mathcal{T}+h)}{(1+R_0)(1+R_2)-R_1^2}, \\ q = \frac{(1+R_0)(\mathcal{T}+h)-R_1(\mathcal{S}+v)}{(1+R_0)(1+R_2)-R_1^2}. \end{cases}$$

where $R_m = \sum_j j^m$, $\mathcal{S}_{\underline{n}} = \sum_j \log_2 \mathcal{L}_{j,\underline{n}}$, and $\mathcal{T}_{\underline{n}} = \sum_j j \log_2 \mathcal{L}_{j,\underline{n}}$.

Proof: Rely on the closed form of

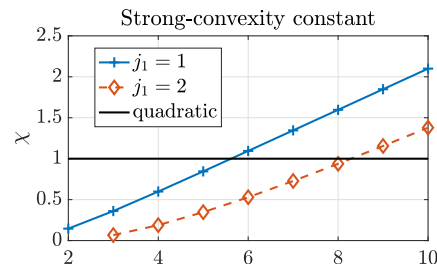
$$\begin{pmatrix} p_{\underline{n}} \\ q_{\underline{n}} \end{pmatrix} = \text{prox}_{\frac{1}{2}\|\Phi \cdot - \log_2 \mathcal{L}_{\underline{n}}\|_2^2} \begin{pmatrix} v_{\underline{n}} \\ h_{\underline{n}} \end{pmatrix} = (\Phi^* \Phi + \text{Id})^{-1} \left(\Phi^* \log_2 \mathcal{L}_{\underline{n}} + \begin{pmatrix} v_{\underline{n}} \\ h_{\underline{n}} \end{pmatrix} \right)$$

with $\Phi = \begin{pmatrix} 1 & 1 \\ 1 & 2 \\ \vdots & \vdots \\ 1 & J \end{pmatrix}$ and thus $\begin{cases} \Phi^* \Phi = \begin{pmatrix} R_0 & R_1 \\ R_1 & R_2 \end{pmatrix} \\ \Phi^* \log_2 \mathcal{L}_{\underline{n}} = \begin{pmatrix} \mathcal{S}_{\underline{n}} \\ \mathcal{T}_{\underline{n}} \end{pmatrix} \end{cases}$

Focus on the data-fidelity term

Strongly convex data fidelity f [Pascal, P., Abry, 2021] [Briceño-Arias, P., , 2022]

Function $f(v, h; \mathcal{L})$ is μ -strongly convex w.r.t the variables (v, h) , with $\mu = \chi$ where $\chi > 0$ is the lowest eigenvalue of the symmetric and positive definite matrix $\Phi^* \Phi = \begin{pmatrix} R_0 & R_1 \\ R_1 & R_2 \end{pmatrix}$ where $R_m = \sum_j j^m$.



Focus on the data-fidelity term

Expression of the conjugate of f [Pascal, P., Abry, 2021]

$$f^*(v, h; \mathcal{L}) = \frac{1}{2} \langle (v, h)^\top, \mathbf{J}^{-1}(v, h)^\top \rangle + \langle (\mathcal{S}, T)^\top, \mathbf{J}^{-1}(v, h)^\top \rangle + \mathcal{C},$$

where

$$\begin{cases} \mathcal{C} &= \frac{1}{2} \langle (\mathcal{S}, T)^\top, \mathbf{J}^{-1}(\mathcal{S}, T)^\top \rangle - \frac{1}{2} \sum_j (\log_2 \mathcal{L}_j)^2. \\ \mathcal{S} &= \sum_j \log_2 \mathcal{L}_j \\ \mathcal{T} &= \sum_j j \log_2 \mathcal{L}_j \\ \mathbf{J} &= A^* A = \begin{pmatrix} R_0 & R_1 \\ R_1 & R_2 \end{pmatrix} \quad \text{and} \quad R_m = \sum_j j^m, \end{cases}$$

(Parameter-free and fast) texture segmentation

PLOVER: Piecewise constant LOcal VariancE and Regularity estimation [Pascal, P., Abry, ACHA, 2021]

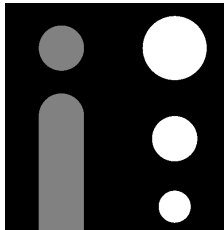
$$\text{Find } (\hat{v}, \hat{h}) \in \underset{v, h}{\operatorname{Argmin}} \sum_j \|\log_2 \mathcal{L}_j - v - jh\|_2^2 + \lambda \underbrace{\|[\Psi v; \alpha \Psi h]^\top\|_{2,1}}_{\text{TV}_\alpha}$$

where TV_α couples spatial variations of v and h and thus favor their occurrences at same location.

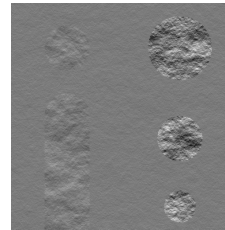
- + Combined estimation and segmentation.
- + Joint estimation of the local variance and local regularity.
- + Strongly convex, closed form expression of the proximity operator associated to the data-fidelity term, Dual formulation possible.

→ **Fast implementation:** Accelerated strongly convex Chambolle-Pock algorithm or FISTA on the dual.

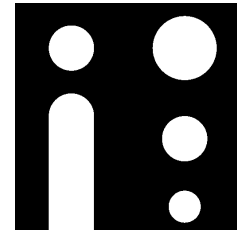
(Parameter-free and) fast texture segmentation



Mask



Synthetic texture



Optimal solution



Parameter-free and fast texture segmentation

→ **Minimization problem:**

$$(\hat{h}, \hat{v}) \in \operatorname{Argmin}_{h,v} \sum_j \|v + jh - \log_2 \mathcal{L}_j\|_2^2 + \lambda \|[\Psi h; \alpha \Psi v]^\top\|_{2,1}$$

→ **Parameter-free:**

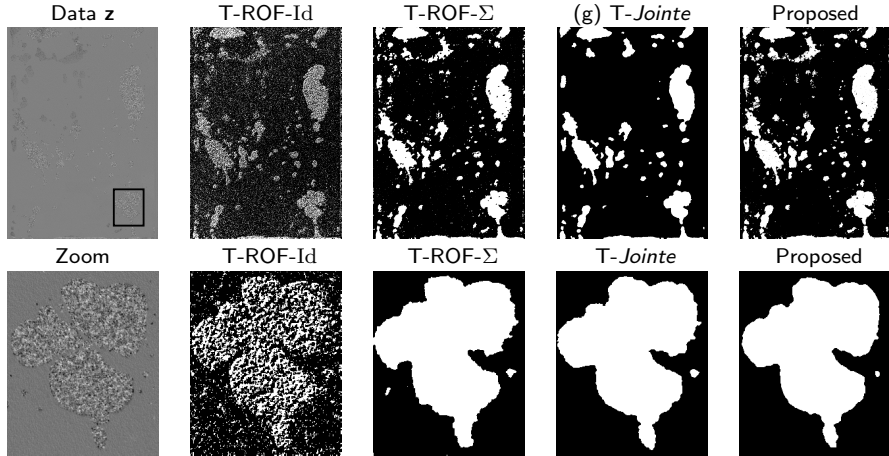
Automatic hyperparameter tuning based on FDMC SURE and FDMC SUGAR with **correlated noise and full rank matrice.** [Deledalle et al., 2014] [Pascal, Pustelnik, Abry, Géminard, Vidal, 2019]

$$\mathbb{E}\|\hat{\mathbf{x}}(\mathbf{z}; \lambda) - \bar{\mathbf{x}}\|^2 = \lim_{\nu \rightarrow 0} \mathbb{E}_{\epsilon, \varepsilon} \hat{R}_{\nu, \varepsilon}(\mathbf{z}; \lambda | \sigma).$$

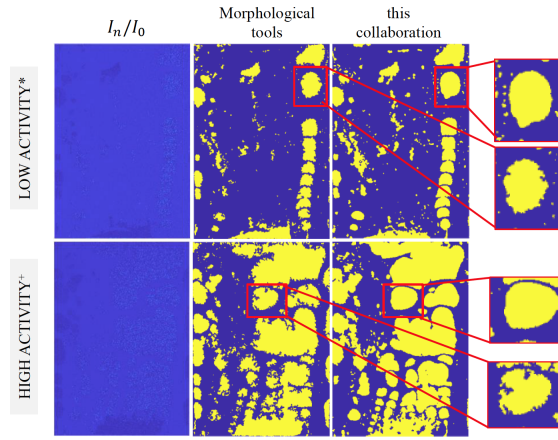
where

$$\hat{R}_{\nu, \varepsilon}(\mathbf{z}; \lambda | \sigma) = \|\hat{\mathbf{x}}(\mathbf{z}; \lambda) - \mathbf{z}\|_2^2 + \frac{2\sigma^2}{\nu} \langle (\hat{\mathbf{x}}(\mathbf{z} + \nu\varepsilon; \lambda) - \hat{\mathbf{x}}(\mathbf{z}; \lambda)), \varepsilon \rangle - \sigma^2 N,$$

Parameter-free and fast texture segmentation



Parameter-free and fast texture segmentation



* $(Q_G, Q_L) = (300, 300)$ mL/min + $(Q_G, Q_L) = (1200, 300)$ mL/min